

Semi-Automated Annotation of Discrete States in Large Video Datasets

Lex Fridman

Massachusetts Institute of Technology
fridman@mit.edu

Bryan Reimer

Massachusetts Institute of Technology
reimer@mit.edu

Abstract

We propose a framework for semi-automated annotation of video frames where the video is of an object that at any point in time can be labeled as being in one of a finite number of discrete states. A Hidden Markov Model (HMM) is used to model (1) the behavior of the underlying object and (2) the noisy observation of its state through an image processing algorithm. The key insight of this approach is that the annotation of frame-by-frame video can be reduced from a problem of labeling every single image to a problem of detecting a transition between states of the underlying object being recorded on video. The performance of the framework is evaluated on a driver gaze classification dataset composed of 16,000,000 images that were fully annotated through 6,000 hours of direct manual annotation labor. On this dataset, we achieve a 13x reduction in manual annotation for an average accuracy of 99.1% and a 84x reduction for an average accuracy of 91.2%.

1 Introduction and Related Work

The biggest of “big data” is video (Mayer-Schönberger and Cukier 2013). 300 hours of video are uploaded to YouTube every minute and, in 2014, YouTube and Netflix accounted for 50% of all peak period downstream traffic in North America (Liu et al. 2015). Like most big data, video is largely unstructured, unlabeled, and unprocessed. However, the proven effectiveness of supervised machine learning in image processing in the last 15 years has shown promise that computer vision can help automate the process of interpreting the content of big video data (Jordan and Mitchell 2015).

As the availability of large-scale video datasets has become widespread over the past decade, semi-automated annotation of images and videos has received considerable attention in computer vision literature (Yuen et al. 2009; Kavasidis et al. 2012). In the image domain, the focus has been on segmenting the image into distinct entities and assigning multiple semantic labels to each entity (Ivasic-Kos, Ipscic, and Ribaric 2015). In the video domain, the focus has been on labeling segmented entities in select keyframe images from the video and propagating the annotation in the keyframes to the frames in-between via linear interpolation, tracking, or time-based regularization (Bianco et al. 2015).

Multi-label annotation and tracking are ambitious and complex efforts that are essential for a general video interpretation framework. Our paper focuses on a narrow but important subset of video data: where a single object is being recorded and that object can be labeled as belonging to one of a finite number of discrete states. We propose a novel framework for semi-automated annotation of that type of video. The two key aspects of our approach is: (1) we reduce the problem of video annotation into change detection and (2) we form a Hidden Markov Model (HMM) for the changes between the states in order to predict when a sequence of classifier decisions correspond to a sequence of stable state self-transitions.

The proposed semi-automated video annotation framework is evaluated on 16,000,000 video-frames of driver faces collected over 150 hours of field driving. The classification of driver gaze regions is an area of increasing relevance in the pursuit of accident reduction. The allocation of visual attention away from the road has been linked to accident risk (Victor et al. 2014) and a drop in situational awareness as uncertainty in the environment increases (Senders et al. 1967).

The problem of gaze tracking from monocular video has been investigated extensively across many domains (Gaur and Jariwala 2014; Sireesha, Vijaya, and Chellamma 2013). We chose driver gaze classification as the case study for the proposed framework for two reasons. First, gaze tracking from video in the driving context is a difficult problem due especially to rapidly varying lighting conditions. Other challenges, common to other domains, include unpredictability of the environment, presence of eyeglasses or sunglasses occluding the eye, partial occlusion of the pupil due to squinting, vehicle vibration, image blur, poor video resolution, etc. We consider the challenging case of uncalibrated monocular video because it has been and continues to be the most commonly available form of video in driving datasets due to low equipment and installation costs. Second, we have 150 hours of double annotated and mediated data. This allows us to evaluate the key trade-off of the semi-automated annotation problem: the reduction in human effort and the classification accuracy achievable under that reduction. The tradeoff curve we present at the end of the paper shows a 13x reduction in human effort for an average accuracy of 99.1% and a 84x reduction for an average accuracy of 91.2%. This improves

significantly on the best result from a similar domain of head pose estimation where 3.3x reduction of manual effort and an accuracy of 97% was achieved on a set 108,000 images (Demirkus, Clark, and Arbel 2014). The strengths and drawbacks of the proposed approach can be summarized as follows:

Strengths

1. **Novel approach to video annotation:** To the best of our knowledge, ours is the first semi-automated discrete state annotation method in video. The key contribution of our work is this idea itself: simplify the problem of video annotation into two problems: (1) discrete object state classification and (2) change detection. In many computer vision application domains these two individual problems have well-developed robust, accurate solutions.
2. **Novel approach to gaze classification:** A lot of work has been done on gaze estimation and classification, but to the best of our knowledge, temporal estimation of gaze regions as a set of discrete states with detectable state transitions has not been done before. That’s why gaze classification was the chosen case study. We believe that many other video analysis applications are similar to it and could be improved with this approach.
3. **State-of-the-art performance:** With the change detection method, to the best of our knowledge, we achieve the best gaze classification results on any large in-the-wild datasets to date.
4. **Dataset size:** The 16,000,000 image evaluation dataset is, by 2 orders of magnitude, the largest annotated gaze dataset we are aware of. We seek to show that this provides a vision for large ever-growing datasets where supervised learning can truly shine.

Drawbacks

1. **Theoretical bounds:** There are no theoretical guarantees on the performance of the overall framework. This is a fundamental shortcoming of an approach that uses supervised learning methods. It relies on the ability of the two underlying classification algorithms to generalize sufficiently well over the data to be of assistance to the human annotator on labeling future data. We will make clear in the paper that the framework makes no guarantees on performance.
2. **Parameters:** There are several parameters in the framework with no automated way of tuning those parameters for a specific domain. This is a big drawback of many learning approaches for real-world datasets. In our empirical evaluation (as shown in Fig. 5), the choices of parameters never resulted in significantly sub-Pareto-optimal performance, but same as in drawback #1, no provable guarantees can be provided.

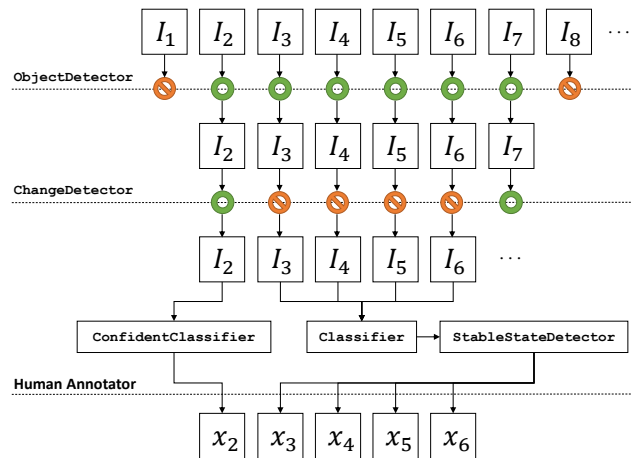


Figure 1: Illustrative diagram of the semi-automated annotation pipeline. The input of the pipeline are the video frames at the top and the output of the pipeline is the per-frame classification of object state at the bottom. The ObjectDetector and ChangeDetector produce binary $\{0, 1\}$ outputs which are indicated in the diagram as crossed-circles for 0 and empty circles for 1.

2 Semi-Automated Annotation Framework

2.1 State Model and Stable State Detection

The video to be annotated is assumed to be of an object that can be labeled at any moment in time as in one instance of state space S . We formulate the dynamics of this discrete state system and its annotation as a Hidden Markov Model (HMM) (Rabiner and Juang 1986). The hidden state is the correct classification of every video frame. The observed output is the estimated class of the image according to the intermediate steps of the pipeline described in §2.2.

During the annotation process, we continually update initial probabilities π_i of being in state i and transition probabilities $a_{i,j}$ of transitioning from state i to state j . Given the observed classifier decisions y_1, \dots, y_m , the most likely state sequence x_1, \dots, x_m that produces the observed decisions is given by:

$$\begin{aligned} V_{1,k} &= P(y_1 | k) \cdot \pi_k \\ V_{t,k} &= \max_{x \in S} (P(y_t | k) \cdot a_{x,k} \cdot V_{t-1,x}) \end{aligned} \quad (1)$$

where $V_{t,k}$ is the probability of the most probable state sequence responsible for the first t observations that have k as its final state. This recurrence relation is used to compute the Viterbi path (Shinghal and Toussaint 1980), the most likely sequence of states that results in the observed classifier decisions. We denote the probability of the Viterbi path as V^* .

The probability that a set of observations is associated with a sequence of unchanged hidden states, assuming the first and state is k is given by:

$$\begin{aligned} V_{1,k} &= P(y_1 | k) \\ V_{t,k} &= P(y_t | k) \cdot a_{k,k} \cdot V_{t-1,k} \end{aligned} \quad (2)$$

The probability of an unchanged sequence of hidden states k normalized by V^* is denoted by V^u . This value is used in §2.2 to determine whether to pass the set of images associated with the sequence of observed classifier decision to the human annotator.

2.2 Semi-Automated Annotation Pipeline

Given a sequences of temporally-adjacent images I_t for $t \in 1, \dots, T$, the annotation pipeline detail in this section and illustrated in Fig. 1 produces hidden state predictions x_t for $t \in 1, \dots, T$. We first describe each of the five component algorithms, and then specify how they are incorporated in the annotation framework.

- **ObjectDetector:** $I_t \rightarrow \{0, 1\}$
Given a single image, this algorithm provides a binary decision on whether the object of interest is present in the image (value of 1) or is absent in the image (value of 0). In the case of gaze classification, this algorithm is a face detector.
- **Classifier:** $I_t \rightarrow S$
Given a single image, this algorithm provides a classification of what hidden state $i \in S$ the object in the image is in.
- **ConfidentClassifier:** $I_t, c_{\min} \rightarrow S$
Given a single image and a confidence threshold c_{\min} , this algorithm provides a classification of what hidden state $i \in S$ the object in the image is in if the classification is above a confidence threshold. The purpose of this algorithm is to replace the human in cases when a confident classification decision can be made.
- **ChangeDetector:** $I_{t-1}, I_t, \delta_{\min} \rightarrow \{0, 1\}$ Give an image at time t and an image immediately before it, this algorithm provides a binary decision on whether a change of state is detected in the image at time t . The change detector uses the threshold δ_{\min} to convert the continuous change detector output to a binary decision.
- **StableStateDetector:**
 $\{I_1, I_2, \dots, I_T\}, V_{\min}^u \rightarrow \{0, 1\}$
Given a temporally-adjacent sequence of images and a likelihood threshold V_{\min}^u , this algorithm makes a decision on whether the sequences of images correspond to a sequence on unchanged hidden states (see §2.1).

The three parameters which control the behavior of the framework are the change detector threshold δ_{\min} , the classifier confidence threshold c_{\min} , and the stable state detector threshold V_{\min}^u . Changing these values results in various points along the tradeoff in human effort and classification effort show in the parametric plot in Fig. 5.

As illustrated in Fig. 1, the above specified algorithms are incorporated in the following data flow:

1. **Sequence Segmentation:** The video data is segmented into continuous sequences of images where the `ObjectDetector` successfully detects the object of interest.
2. **Change Detection and Classification:** Detect the changes in the image sequences using

`ChangeDetector` and the threshold c_{\min} . Use `ConfidentClassifier` to classify each of the 2 images before and after the detected change. If no confident classification can be made, these 5 images (2 prior, 1 current, and 2 subsequent images) are sent to the manual annotation queue.

3. **Change Verification:** If two adjacent change-points do not share a connecting state, all of the images between the two change-points are sent to the manual annotation queue.
4. **Stable State Detection:** Classify each state between the detected changes using the `Classifier`. These classification decisions are the observations of the HMM described in §2.1. If the normalized probability V^u of an unchanged state is above the threshold V_{\min}^u , then the states between the two detected changes are labeled according to the estimated hidden state.
5. **Human Annotation:** Any images added to the manual annotation queue in the previous 4 steps are double annotated and mediated by a human.

The performance of the overall system depends on the accuracy of each of the five algorithms defined above. As the annotation process proceeds, the manually annotated images should be frequently used to re-train each of the algorithms.

3 Case Study: Driver Gaze Classification

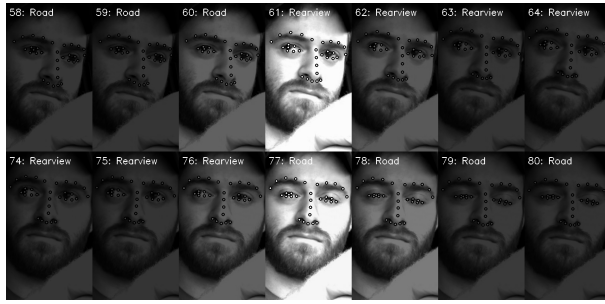
3.1 Dataset

Evaluation of the semi-automated annotation framework is carried out on a dataset of 150 hours of video data spanning 244 different drivers traversing over 10,000 miles of highway. For each subject, the collection of data was carried out in one of a set of study vehicles: 2013 Chevrolet Equinox, 2013 Volvo XC60, 2014 Chevy Impala, or 2014 Mercedes CLA (randomly assigned). The data was double manually annotated of driver glances transitions during secondary task periods (at a resolution of sub-200ms) into one of 11 classes (road, center stack, instrument cluster, rearview mirror, left, right, left blindspot, right blindspot, passenger, uncodable, and other). Any discrepancies between the two annotators were mediated by an arbitrator.

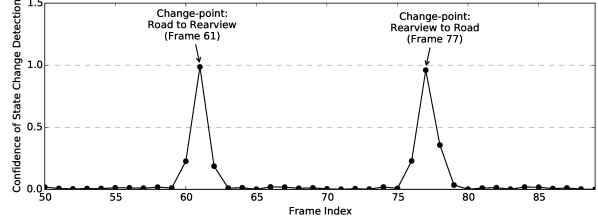
3.2 Gaze Classification and Change Detection

The application of the framework described in §2 requires the definition of `ObjectDetector`, `Classifier`, `ConfidentClassifier`, `ChangeDetector`, and `StableStateDetector` specific to the gaze classification problem. We consider the problem of classifying driver gaze into six regions: Road, Center Stack, Instrument Cluster, Rearview Mirror, Left, and Right. These six region forms the state space S for the HMM in the implementation of the `StableStateDetector` algorithm.

Face Detection For the gaze classification problem, the object is the human face, and so the `ObjectDetector` algorithm is a face detector. The environment inside the car is relatively controlled in that the camera position is fixed and the driver torso moves in a fairly contained space. Thus,



(a) Two sequences of images showing a state transition (1) from “Road” to “Rearview Mirror” and (2) from “Rearview Mirror” to “Road”. The transparency of the image (over a black background) is proportional to the value produced by the change detection classifier. The bright image in the middle of each sequence is the one predicted to be where the state transition occurred.



(b) The output of the change detection classifier where a value of 1 means a change-point was detected and a value of 0 means a no change-point was detected. The x-axis of this plot corresponds to the frame indices marked in each image above the plot.

Figure 3: Representative example of the change detection algorithm output on two sequences of images.

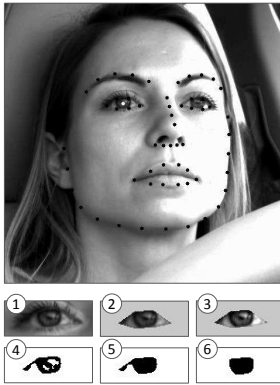


Figure 2: Example of facial landmark alignment and the intermediate steps of the pupil detection. The black dots designate the landmarks and the single white dot designates the pupil position in the right eye. Below the image of the face image are 6 steps of the pupil detection.

a camera can be positioned such that the driver’s face is always fully or almost fully in the field of view. The face detector in our pipeline uses a Histogram of Oriented Gradients (HOG) combined with a linear SVM classifier.

Feature Extraction The steps in the gaze region classification pipeline are: (1) face alignment, (2) pupil detection, (3) feature extraction and normalization, and (4) classification. The face image in Fig. 2 is an example of the result achieved in the first three steps of the pipeline: going from a raw video frame with a detected face to extracted face features and pupil position. The relative orientation of facial features serves as a proxy for “head pose” and the relative orientation of pupil position serves as a proxy for “eye pose”. We discuss each of the six steps in the pipeline in the following sections.

Face alignment in our pipeline is performed on a 68-point Multi-PIE facial landmark mark-up used in the iBUG 300-

W dataset (Sagonas et al. 2013). These landmarks include parts of the nose, upper edge of the eyebrows, outer and inner lips, jawline, and parts in and around the eye. The selected landmarks are shown as black dots in Fig. 2. The algorithm for aligning the 68-point shape to the image data uses a cascade of regressors as described in (Kazemi and Sullivan 2014) and implemented in (King 2009).

The problem of accurate pupil detection is more difficult than the problem of accurate face alignment, but both are not always robust to poor lighting conditions. Therefore, the secondary task of pupil detection is to flag errors in the face alignment step that preceded it. The face is detected in 79.4% video frames but only 61.6% of the original frames pass the pupil detection step.

We use a CDF-based method (Asadifard and Shanbezaheh 2010) to extract the pupil from the image of the right eye, and adjust the extracted pupil blob using morphological operations of erosion and dilation. The six steps in this process are as follows:

1. Extract the right eye from the face image based on the right eye features computed as part of the face alignment step.
2. Remove all pixels that fall outside the boundaries of the polygon defined by the 6 eye features.
3. Rescale the intensity such that the 98-percentile intensity becomes 1.0 intensity and 2-percentile intensity becomes 0.0 intensity.
4. Define a CDF intensity threshold and convert the grayscale image to a binary image. Each pixel intensity above the threshold becomes 1, and otherwise becomes 0.
5. Perform an “opening” morphology transformation. This operation is useful for removing small holes in large blobs.
6. Perform a “closing” morphology transformation. This operation is useful for removing small objects and smoothing the shape of large blobs.

The above steps have three parameters: the CDF threshold, the opening window size, the closing window size. These parameters are dynamically optimized for each image over a discrete set of values in order to maximize the size of the largest resulting blobs under one constraint: the largest blob must be circle-shaped (i.e. have similar height and width).

Classification and Decision Pruning A random forest classifier is used to generate a set of probabilities for each class from a single feature vector. The probabilities are computed as the mean predicted class probabilities of the trees in the forest. The class probability of a single tree is the fraction of samples of the same class in a leaf. A random forest classifier of depth 25 with an ensemble of 2,000 trees is used for all experiments in §3.3. The class with the highest probability is the one that the system assigns to the image as the “decision”. The ratio of the highest probability to the second highest probability is termed the “confidence” of the decision. A confidence of 1 is the minimum. There is no maximum. This algorithm is used to define the `Classifier` and `ConfidentClassifier` algorithms with the confidence threshold set to 1 and 10, respectively.

Change and Stable State Detection The `ChangeDetector` algorithm for gaze classification uses a depth 15, 1000-tree random forest classifier based on the following four features computed from the change between two images:

1. Average of dense optical flow over the bounding box of the eyes and the nose.
2. Average of dense optical flow over the bounding box of each eye.
3. Change in position of landmarks for the eyes and the nose.
4. Change in pupil position.

The random forest classifier produces a confidence score that the image is associated with a change of state based on the fraction of decision trees that predicted the image belongs to the “change” class. This score is compared with the threshold to make the binary change detection decision. A representative image sequence and resulting change detector output for each image is shown in Fig. 3.

3.3 Results

The evaluation of the gaze classification and change detection algorithms in the semi-automated annotation framework was carried out on the 16 million video-frame dataset (see §3.1). The classifiers were “seeded” by assuming that 20,000 images were first manually annotated. Then, the algorithm detailed in §2.2 was followed until all images were annotated by human or machine. The re-training of the classifier models was performed every 20,000 manually annotated images. The confusion matrices in Fig. 4 show the classification accuracy achieved by `Classifier` and `ConfidentClassifier` algorithms given default values of parameters δ_{\min} , c_{\min} , and V_{\min}^u . The confusion matrix for `Classifier` forms the conditional observation probabilities in (1) and (2).

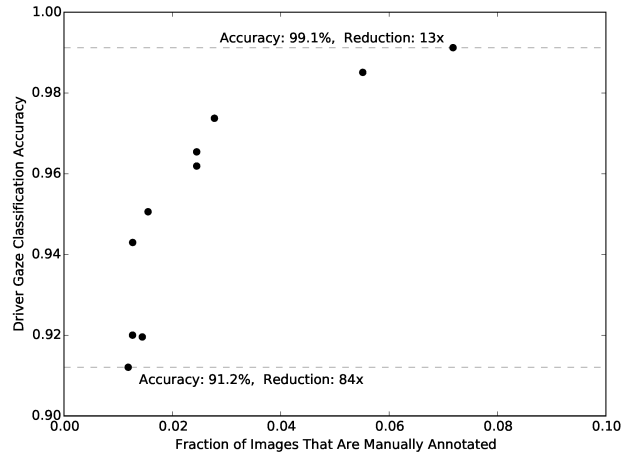


Figure 5: Parametric plot showing the empirical tradeoff between savings in human annotation effort and the accuracy of the resulting annotation. The biggest observed savings are an 84x reduction in human effort resulting in 91.2% annotation accuracy. The highest accuracy of 99.1% was associated with a 13x reduction in human effort.

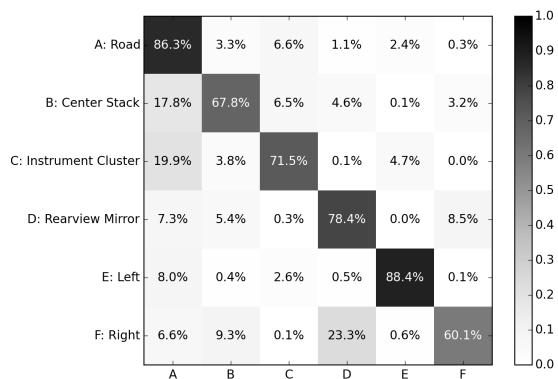
The parametric plot in Fig. 5 shows the reduction in manual effort and annotation accuracy achieved by varying the change detect threshold δ_{\min} from 0.1 to 0.5. The former value results in a 84x reduction and annotation accuracy of 91.2%. The latter value results in a 13x reduction and annotation accuracy of 99.1%.

4 Conclusion

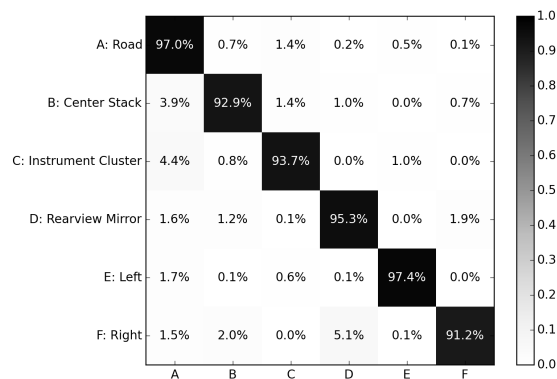
We consider the problem of annotating video of an object that can be labeled as being in one of a finite set of discrete states. The goal of the proposed solution is to significantly reduce the human effort component of the annotation. The key insight of our approach is that we can reduce the annotation problem to a change detection problem. The performance of the framework is evaluated on a driver gaze classification dataset composed of 16,000,000 images that were fully annotated over 6,000 hours of direct manual annotation labor. We present a tradeoff in human effort savings and final annotation accuracy on this dataset, showing a 13x reduction in manual annotation for an average accuracy of 99.1% and a 84x reduction for an average accuracy of 91.2%.

References

- [Asadifard and Shanbezadeh 2010] Asadifard, M., and Shanbezadeh, J. 2010. Automatic adaptive center of pupil detection using face detection and cdf analysis. In *Proceedings of the International MultiConference of Engineers and Computer Scientists*, volume 1, 3.
- [Bianco et al. 2015] Bianco, S.; Ciocca, G.; Napoletano, P.; and Schettini, R. 2015. An interactive tool for manual, semi-automatic and automatic video annotation. *Computer Vision and Image Understanding* 131:88–99.



(a) Classifier with average accuracy of 75.4%.



(b) ConfidentClassifier with average accuracy of 94.6%.

Figure 4: Confusion matrices for the six-region classification problem. The gaze regions are: road, center stack, instrument cluster, rearview mirror, left, and right.

[Demirkus, Clark, and Arbel 2014] Demirkus, M.; Clark, J. J.; and Arbel, T. 2014. Robust semi-automatic head pose labeling for real-world face video sequences. *Multimedia Tools and Applications* 70(1):495–523.

[Gaur and Jariwala 2014] Gaur, R. P., and Jariwala, K. N. 2014. A survey on methods and models of eye tracking, head pose and gaze estimation. In *Journal of Emerging Technologies and Innovative Research*, volume 1. JETIR.

[Ivasic-Kos, Ipsic, and Ribaric 2015] Ivasic-Kos, M.; Ipsic, I.; and Ribaric, S. 2015. A knowledge-based multi-layered image annotation system. *Expert Systems with Applications*.

[Jordan and Mitchell 2015] Jordan, M., and Mitchell, T. 2015. Machine learning: Trends, perspectives, and prospects. *Science* 349(6245):255–260.

[Kavasidis et al. 2012] Kavasidis, I.; Palazzo, S.; Di Salvo, R.; Giordano, D.; and Spampinato, C. 2012. A semi-automatic tool for detection and tracking ground truth generation in videos. In *Proceedings of the 1st International Workshop on Visual Interfaces for Ground Truth Collection in Computer Vision Applications*, 6. ACM.

[Kazemi and Sullivan 2014] Kazemi, V., and Sullivan, J. 2014. One millisecond face alignment with an ensemble of regression trees. In *Computer Vision and Pattern Recognition (CVPR), 2014 IEEE Conference on*, 1867–1874. IEEE.

[King 2009] King, D. E. 2009. Dlib-ml: A machine learning toolkit. *Journal of Machine Learning Research* 10:1755–1758.

[Liu et al. 2015] Liu, Y.; Blasiak, S.; Xiao, W.; Li, Z.; and Chen, S. 2015. A quantitative study of video duplicate levels in youtube. In *Passive and Active Measurement*, 235–248. Springer.

[Mayer-Schönberger and Cukier 2013] Mayer-Schönberger, V., and Cukier, K. 2013. *Big data: A revolution that will transform how we live, work, and think*. Houghton Mifflin Harcourt.

[Rabiner and Juang 1986] Rabiner, L. R., and Juang, B.-H. 1986. An introduction to hidden markov models. *ASSP Magazine, IEEE* 3(1):4–16.

[Sagonas et al. 2013] Sagonas, C.; Tzimiropoulos, G.; Zafeiriou, S.; and Pantic, M. 2013. 300 faces in-the-wild challenge: The first facial landmark localization challenge. In *Computer Vision Workshops (ICCVW), 2013 IEEE International Conference on*, 397–403. IEEE.

[Senders et al. 1967] Senders, J. W.; Kristofferson, A.; Lev-ison, W.; Dietrich, C.; and Ward, J. 1967. The attentional demand of automobile driving. *Highway research record* (195).

[Shinghal and Toussaint 1980] Shinghal, R., and Toussaint, G. T. 1980. The sensitivity of the modified viterbi algorithm to the source statistics. *Pattern Analysis and Machine Intelligence, IEEE Transactions on* (2):181–185.

[Sireesha, Vijaya, and Chellamma 2013] Sireesha, M.; Vijaya, P.; and Chellamma, K. 2013. A survey on gaze estimation techniques. In *Proceedings of International Conference on VLSI, Communication, Advanced Devices, Signals & Systems and Networking (VCASAN-2013)*, 353–361. Springer.

[Victor et al. 2014] Victor, T.; Dozza, M.; Bärgrman, J.; Boda, C.-N.; Engström, J.; and Markkula, G. 2014. *Analysis of Naturalistic Driving Study Data: Safer Glances, Driver Inattention, and Crash Risk*.

[Yuen et al. 2009] Yuen, J.; Russell, B.; Liu, C.; and Torralba, A. 2009. Labelme video: Building a video database with human annotations. In *Computer Vision, 2009 IEEE 12th International Conference on*, 1451–1458. IEEE.